

# Numerical and tank test of a pivoted floating device for wave energy

In this paper a system for extracting energy from waves is presented. The present work deals with numerical and experimental tests on a scaled model, performed in the DII towing tank facility. The device is made up of a floating body, which oscillates due to waves, and of a linear electromechanical generator. The electromechanical generator, based on ball-bearing screw, is linked both to the buoyant body and a fixed frame, converting relative movements of its anchor point in electrical power. Numerical analyses on such device have been performed in order to evaluate critical parameters for the system optimization, including analytical study of the system, potential flow and computational fluid dynamics (CFD) simulations, based on Reynolds Averaged Navier-Stokes (RANS), as well.

DOI: 10.12910/EAI2015-039

■ D.P. Coiro, G. Troise, G. Calise, N. Bizzarrini

## Introduction

The new trends in the field of renewable energy are to enhance the extraction of energy from waves. This kind of renewable source represents an interesting field of investigation for its numerous recognized advantages: these are related to its relatively limited environmental impact and more predictable behavior with respect to other energy sources, making it a very attractive feature for energy systems design. In particular, ocean waves often show relatively repeatable amplitude and frequency characteristics, which depends on the specific installation site.

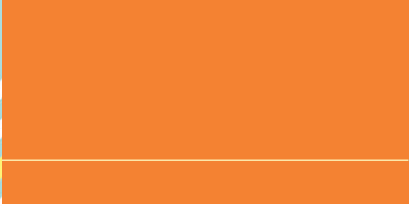
In the design of wave energy system, many configuration parameters are involved: buoyant body shape, overall system arrangement and conversion

system device are some important key-features. This kind of system is mainly intended for installation in suitable sea coastal areas. Generally speaking, operating principle ensures ease of construction and operation; but, on the other hand, an adequate conversion system has to be developed for converting floating body movements into electrical power.

This work refers to an innovative configuration of such kind of devices, based on an available suitable body shape. The overall system arrangement effects are analyzed in order to optimize the power extraction from waves. In this work, a study of the power performance characteristic of a small-scale model of the system, under different operating conditions, will be presented.

As a starting point, an analytical study for extracting kinematic operating laws is performed; then, computer-aided simulations are performed, both potential flow and Reynolds Averaged Navier-Stokes (RANS). At the end, several towing tank tests are performed to verify data from simulations, better tune-up the engineering process and investigate other device arrangements as well.

■ Contact person: Domenico P. Coiro  
coiro@unina.it



## Wave energy conversion system

In this section, an overall description of the system operating principle will be developed. In Figure 1, the two main configurations investigated are presented: in rest condition, the horizontal arms configuration has the generator, here named PTO (Power Take-Off) device, perpendicular both to arms and free water surface; conversely, the inclined arms configuration, at rest, has the PTO approximately perpendicular only to arms. The rotation of the body is possible thanks to two hinges which are, respectively, above and below the water free surface. During the free motion of the body, the angle between arms and PTO direction changes respect to perpendicular condition.

The dynamic behavior of the system may be described by the use of a 1 DOF equation, that is the equilibrium of moments around the hinge axis:

$$I\ddot{\theta} + B\dot{\theta} + K\theta = M_{ext} + M_{PTO} \quad (1)$$

where:

- $I$  is the rotational inertia around the hinge axis, also accounting for the hydrodynamic added mass;
- $B$  is a linear damping coefficient, accounting for part of the radiation force and which should also include the viscous contribution;
- $K$  is a coefficient related to hydrostatic stiffness;
- $M_{ext}$  is the external moment due to waves;
- $M_{PTO}$  is the moment due to the point-pivoted PTO.

The PTO system was simulated during experiments by means of a controlled pneumatic actuator. The selected PTO system was controlled so as to produce a force response proportional to velocity variations (Eq. 2).

$$P_{inst} = \vec{F} \vec{V} = K\vec{V} \vec{V} \quad (2)$$

The coefficient  $K$  may influence the performance of the system in response to waves and it has become a key parameter for the choice of the electrical conversion system. This parameter may be set to a desired value through a controllable gain, via the

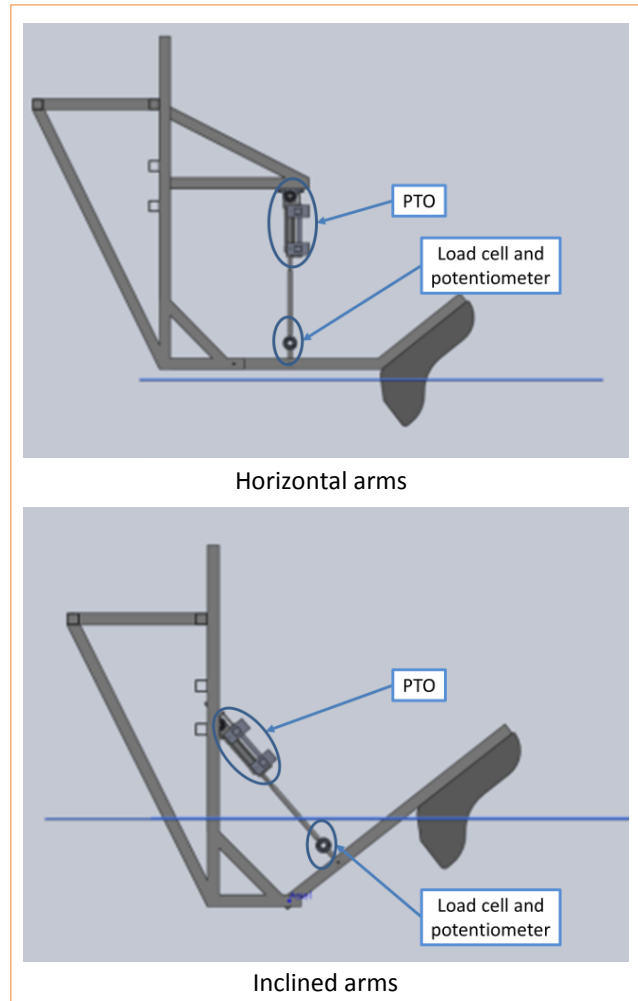


**FIGURE 1** Two tested configurations

actuator control software, in order to test different operating conditions and estimate the optimal condition for power production.

The system power production performances are also evaluated, measuring the PTO's anchor point displacements by means of a potentiometer, and PTO's axial force by means of a load cell: then, the power is indirectly estimated as product of force times velocity. Incident waves are measured by ultrasonic probes. Then, all these measurements are collected and compared with numerical results.

## Towing tank experimental tests

Experimental towing tank tests were made in the facility available at the Department of Industrial Engineering – Naval Div. of the University of Naples. This facility has a wave generator capable of producing waves with variable frequency and amplitude. The wave tank has a length of 140 m, depth of 4.5 m and width of 9 m. For all tests performed, deep water assumption can be made. The main properties of the tested model (Fig. 2) are listed in Table 1.

### Preliminary tests

Some preliminary verification tests were performed in order to determine the effective inertial characteristic of the body and to investigate the effect of hinge friction, which has been considered negligible. Hinge friction

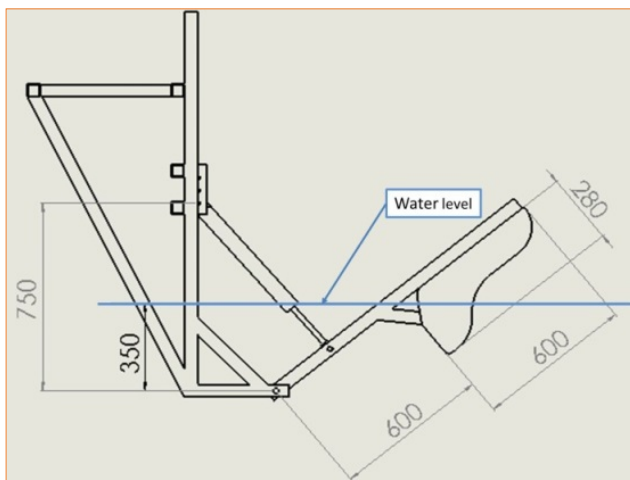


FIGURE 2 Tested model main properties

Scaled Model Properties		
Body height	0.60	m
Body width	1.00	m
Body weight	32.50	kg
Hinge moment (Body + arms)	21.65	Kg·m <sup>2</sup>
Draft	0.20	m
Body section@water level	0.210	m <sup>2</sup>
Immersed volume	0.0325	m <sup>3</sup>

TABLE 1 Scaled Model Properties

measurements have been performed using the buoy as a pendulum, suspended around its hinge axis. Buoyant movements around its equilibrium positions have been measured by a distance-laser measuring system and a typical linear decay in the amplitude oscillation has been observed.

Coulomb friction coefficient, from the observed decaying oscillations, has been evaluated even with different weights added to the buoy. The estimated hinge friction torque was in the range 1.2-2.1 N m, acceptably small for the purposes of the tests even if not negligible.

### Free response from a non-equilibrium initial condition

In this kind of tests, the PTO is not yet installed and response of the system is measured by a potentiometer. The system has been slightly moved from its initial rest condition and kept free to move, for recording the damped response. From response data, in terms of angular displacement, the damping ratio and the damped oscillation period have been estimated, from the exponential decay of the damped free response and from the inertial properties of the body. These results were compared to a simple mass-damper model of similar characteristics (Fig. 3) as well.

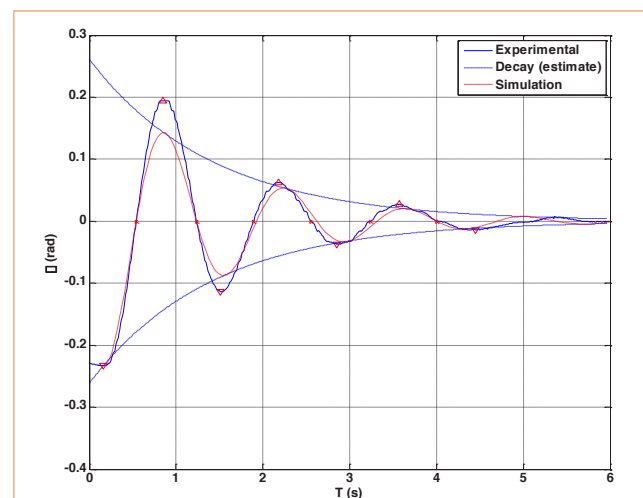
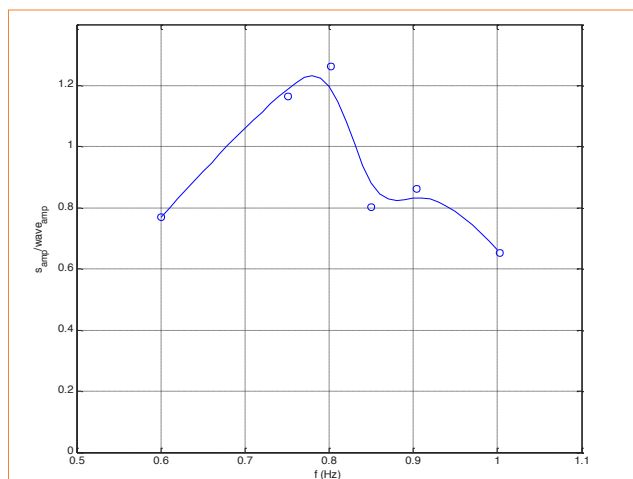


FIGURE 3 Free response test of the floating system (hinged buoy oscillation angle time history)

	Damping ratio	Natural frequency	Added inertia	Damping coefficient (around hinge axis)
	$\zeta$ (-)	$f_n$ (Hz)	$I_a$ (kg·m <sup>2</sup> )	B (N·m·s·rad <sup>-1</sup> )
Mean	0.156	0.767	20.1	62.8
Std. dev.	0.012	0.020	2.146	5.267

**TABLE 2** Damped response characteristics (mean values)



**FIGURE 4** Response operator as piston displacement/wave amplitude ratio, as a function of wave frequency for 3 cm wave amplitude tests (Circles refer to direct experimental results, while the continuous line is a fitting curve)

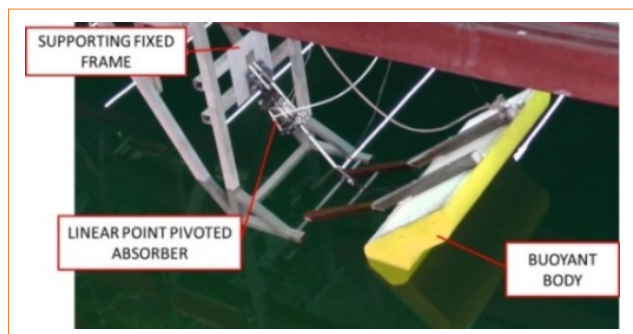


**FIGURE 5** Scaled model for towing tank tests

From these data, other useful information was inferred such as the added inertia or the hydrodynamic damping. Some troubles have been observed in matching the simulated and observed response and these difference may be imputed to the lack of perfect control in the initial conditions imposed in each experimental test: indeed, the system was manually displaced from the equilibrium position and the effective starting conditions was not perfectly controlled, even if the overall behavior is correctly predicted. On the other hand the oscillations are highly damped and the number of observed damped cycles is relatively small, reducing the number of data available for estimation. The mean value of the estimated parameter from all the performed tests is reported in Table 2.

#### **System response to waves without PTO device**

Under waves, the system has been tested under different wave amplitude and frequency conditions. The waves generated were sinusoidal.

A response amplitude operator (RAO) for the system has been experimentally estimated, dividing the linear displacement of the attachment point of the buoy (measured by the potentiometer) by the wave amplitude. These tests have also been performed only with the potentiometer (without PTO). Data collected, in terms of RAO (Fig. 4), show an amplitude peak in the range 0.75–0.8 Hz, in good agreement with free response test results.

#### **Determination of PTO coefficient**

In these tests, time histories of the instantaneous power were recorded under both different wave conditions (amplitude and frequency) and different values of the proportionality coefficient  $K$ . Both configurations in Figure 1 have been tested. The inclined arms model used during tests is shown in Figure 5. The two configurations allow to understand the effect of combined vertical and horizontal components of the forces from waves. The part of the body subject to hydrodynamic interaction is held approximately constant in both configurations. Two different types of actuators have been used during tests: a controlled pneumatic four-quadrant

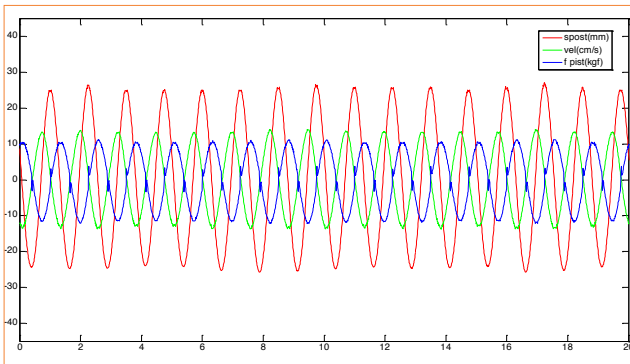


**FIGURE 6** Time histories of measured quantities in a typical test: PTO piston displacement (red), piston force (blue), piston velocity (green). Amplitude  $A = 5$  cm, Frequency  $f = 0.8$  Hz, piston force-speed gain  $K = 800$   $\text{N s m}^{-1}$

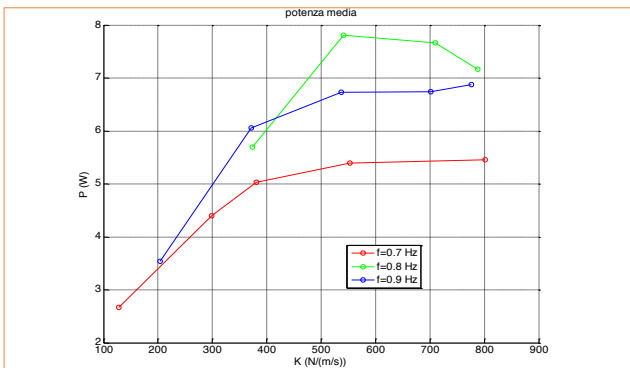


**FIGURE 7** Experimental mean power as a function of piston force-speed gain for different incident wave frequency (5 cm wave amplitude). Inclined arms configuration (with better performance)

actuator, used as a damper, and a passive electric linear generator. A typical set of measured data is reported in Figure 6.

Different tests have been performed using different wave amplitude and frequency and varying the PTO gain  $K$ , in order to identify optimal conditions for energy conversion. The maximum allowable gain  $K$  was limited to about  $800$   $\text{N s m}^{-1}$ . Results are shown in Figure 7 and Figure 8 in terms of mean power. Each point in the figure corresponds to a single test.

For the inclined arms configuration, power output

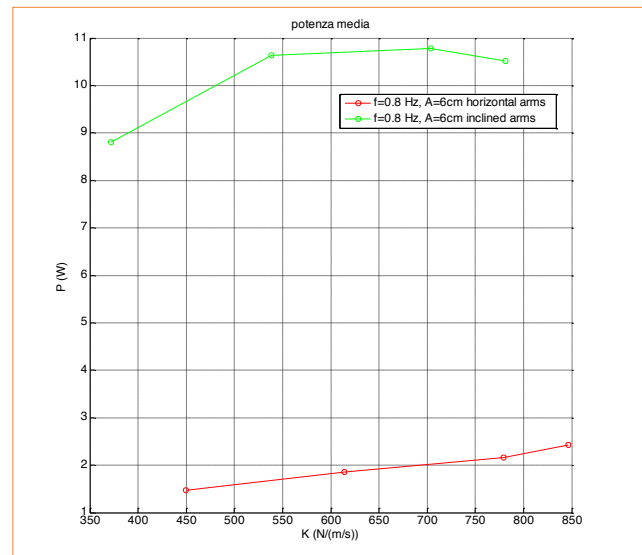


**FIGURE 8** Experimental mean power as a function of piston force gain for fixed incident wave frequency (0.8 Hz) and wave amplitude (6 cm). Comparison of inclined arm configuration (green) with the horizontal one (red)

shows a peak for wave frequency in proximity to system natural frequency; max power output is at a value of the gain  $K$  of approximately  $600$   $\text{N s m}^{-1}$ . For the scaled model, the power peak value is about  $8$   $\text{W}$  for incident wave amplitude of  $5$  cm.

The two tested configurations have shown very different behaviors. The inclined arms configuration seems to be more effective in energy conversion. Probably this is due to the effect of the horizontal component of the hydrodynamic action which, in the inclined arms case, gives a favorable contribution to the moment around the hinge axis (the effective vertical distance between hinge axes and center of buoyancy is greater).

### Wave breaker effect

A wave breaker behind the buoyant system was introduced to verify coastline effects. A small number of tests have been performed to investigate its effect and in only one configuration, with the wall mounted at a distance of about  $2$  m from the hinge axis. As inferred from results, it seems that the horizontal arm configuration was relatively more sensitive to the presence of the wall. The wave breaker influence

depends strongly on the wavelength of the incident wave: the augmented power output is a consequence of a stationary wave system which is established in front of the wall itself and, if the floating body is placed at a peak point in the stationary wave pattern, the power output may be significantly amplified. However, further investigations are needed.

### Potential flow simulations

Potential flow simulations have been performed by the use of a boundary elements code. The dynamic response of the system due to waves is evaluated by estimating the hydrodynamic coefficients and solving the equation of motions. Physical constraints have been simulated as well. Both configurations have been tested and, for each wave frequency, added mass, radiative damping, diffractive and Froude-Krylov forces were recorded.

Numerical preliminary analyses, similar to experimental ones, were performed and free response of the system was evaluated to identify its natural frequency. At a second stage, the PTO effect, by means of its force on the anchor point, was introduced into numerical analyses. Then, other simulations were performed using wave conditions similar to tests for comparing the electrical power

output. The overall dynamic behavior of the numerical model resulted qualitatively similar to the tested ones, in terms of both motion and forces.

Numerical potential flow data have shown a good agreement with experimental tests, regarding the value of natural frequency and wave frequency for max power (both mean and instantaneous); but, absolute values of the electrical power output are almost twice those of the tests. This is probably due to an overestimation of the buoy velocity, since viscous effects weren't accounted in this kind of simulations.

Viscous actions may be accounted into the simulations, introducing a fictitious friction torque around the hinge axis: for some numerical analyses, a value of 10 N m has been used. Using such a constant friction action, output power is reduced and the matching with experimental values is improved, as can be seen in Figure 9.

### Performance optimization

For its quickness and suitability, the potential flow solver can be used for implementing an optimization procedure. Some geometrical parameters, identified as critical ones, mass and immersed volume were changed in order to increase the power extracted from waves. For optimization, each parameter can change in a preset range and a cost function is properly defined. Two different algorithms were used such as NSGA-II and SIMPLEX. Unfortunately, not all the optimization cases were successful, probably due to meshing problem; moreover, only a part of successful ones are feasible.

Optimizations were made on the full-scale model, by means of potential flow solver, and results are summarized in Table 3. In the first attempt, the buoy shape was modified changing only one geometric parameter, a frontal fillet radius of the buoy lateral profile, in addition to mass and PTO coefficient. Despite some fluctuations, results have shown a moderate increment of the average output power. The second attempt was made changing two fillet radiuses, mass and PTO coefficient. In this condition, only a small further increment of the average output is reached. Anyway, the most valuable contribution to power output enhancement seems to be related to the variation of the immersed volume and of the piston force gain. The

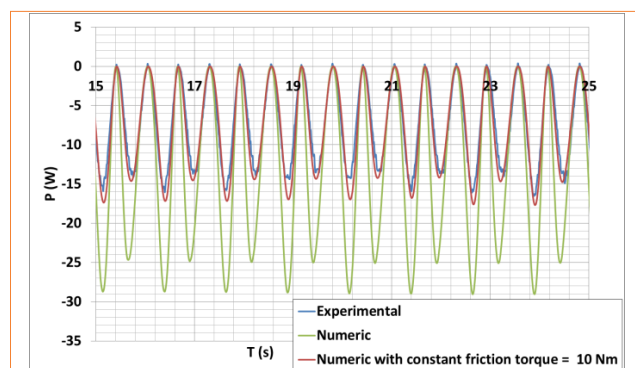


**FIGURE 9** Numerical [potential theory] - experimental comparison. Instantaneous power time histories. [ $A = 0.05$  m,  $f = 0.8$  Hz,  $K \approx -570$  N s  $m^{-1}$ ]. In red the simulation with a fictitious constant friction torque of 10 N m added



	Average Power	Mass	Fillet Radius #1	Fillet Radius #2	PTO Coefficient	Submerged Volume
	$P_{avg}$ (kW)	M (kg)	$R_1$ (m)	$R_2$ (m)	K ( $N \cdot s \cdot m^{-1}$ )	$V_{sub}$ ( $m^3$ )
base	6.2	3780	1.00	0.800	$5.0 \cdot 10^5$	4.00
1	7.4	6940	1.70	-	$8.3 \cdot 10^5$	7.40
2	7.8	7275	1.92	1.433	$7.6 \cdot 10^5$	7.70
3	6.2	3365	1.00	0.810	$3.9 \cdot 10^5$	3.52

**TABLE 3** Optimization results: best cases

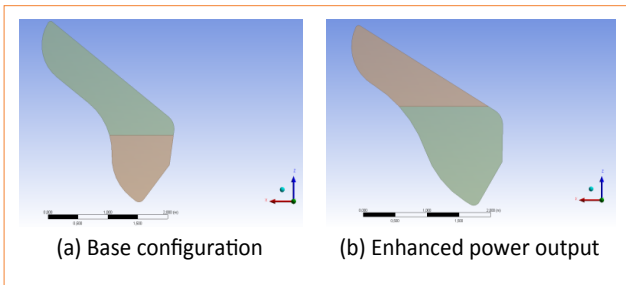


**FIGURE 10** Comparison of optimization results. (The final immersed volume is increased from 4  $m^3$  to 7.7  $m^3$ )

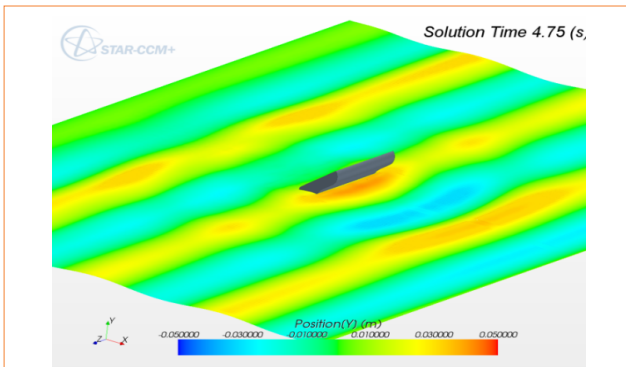


**FIGURE 11** Typical RANS simulation screenshot

last try was made searching for the maximum specific power ( $P_{avg}$  divided by the submerged volume  $V_{sub}$ ). In these first attempts, no effective increment in the power output is reached, even if the initial immersed volume is reduced, and the geometric parameters tend to remain very close to the base configuration (Fig. 10).

## Reynold-Averaged Navier-Stokes Simulations

Computational Fluid Dynamics (CFD) simulations, based on Reynolds-Averaged approach (RANS), were performed on the buoy, without considering supporting arms. CFD was used in the attempt of considering viscous effects as well. Only half of the real physical domain was considered, exploiting the symmetrical properties of the problem. A simulated towing tank was created, in which the buoy can rotate around a simulated hinge: the overlapping mesh approach was used to let the buoy rotate. Mesh sensitivity analysis was done, and a mesh of about 6 million cells, which ensures sufficient accuracy and less CPU time, was chosen. Despite this, each CFD simulation had required about two days on a 64 CPUs device, also for the use of computationally expensive physical models such as Volume-Of-Fluid (VOF) two-phases physics and turbulence model.

RANS simulations (Fig. 11) seemed to reproduce well the overall system dynamics as observed during tests. However, some data from CFD was not in agreement with experimental data. Results of free-response simulations had shown an underestimation of the natural frequency. Data from simulations under wave actions had revealed that maximum power values, both instantaneous and average ones, will occur at the natural frequency predicted by CFD, but it is quite different with respect to reality. Sensitivity of the model about inertia and boundary condition was also analyzed without significant effects. The introduction of other frame structural elements, such as supporting arms, did not produce relevant modifications to critical system parameters.

The PTO system was also accounted in simulations using the Eq. 2: velocity, normal to the supporting arms, is continuously updated during the simulation as the counteracting PTO's action. Then, sensitivity analyses about  $K$  were performed in order to determine its value for higher power extraction.

In the light of this, further investigation have to be made in order to understand how to tune-up and troubleshoot RANS simulation.

## Final remarks

In [2] there are some insights about the definition of the capture width ratio ( $CWR$ ) as:

$$CWR = P_{avg} / P_{wave} B \quad (3)$$

where  $B$  is the width of the body,  $P_{avg}$  the cycle average power output and  $P_{wave}$  is the power amount enclosed in the wave. Based on  $CWR$ , the scaled model shows that for a maximum average power of about 7.8 W with at 5 cm wave amplitude, a  $CWR$  of about 0.65 is reached.

The results here presented, for both numerical analysis and experimental tests on a scale model, represent a suitable base for further investigation. Even if, comparing numerical data with experimental ones, some differences are present (Fig. 12), it can be stated that operating frequency of resonance is captured fairly well by potential flow simulations, but maximum power and average power are significantly overestimated. On the other hand, the peaks of power predicted by RANS simulations are slightly closer to experimental values. Finally, an attempt of optimization procedure has been developed in order to search for an enhanced

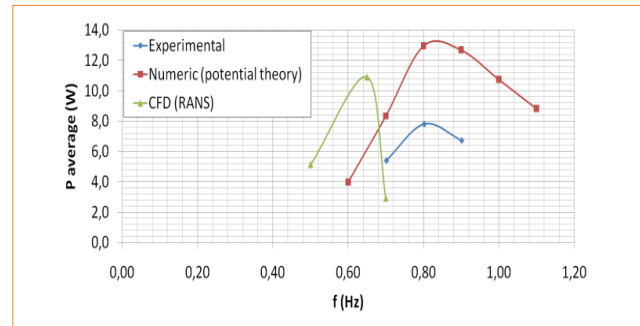


**FIGURE 12** Experimental-numerical comparison (5 cm wave amplitude,  $K \approx 600 \text{ N s m}^{-1}$ )

geometric configuration, using the potential flow solver for its reduced computational cost. Therefore, with all the data and methods developed during this work, it is possible to define a reliable method for predicting performance and designing a wave generator full-scale system, or optimizing an existing device. Just to make an example, 5 m wide full scale prototype with rated power of 60 kW, deployed on West coast of Sardinia in Italy, is capable of producing about 150 MWh of energy per year with an estimated average cost per kW installed of about 2500 Euro.

## Acknowledgements

This work has been done in cooperation with Umbra Group company ([www.umbragroup.it](http://www.umbragroup.it)) which has sponsored the research.

**Domenico P. Coiro, Giuseppe Calise, Nadia Bizzarrini**  
University of Naples "Federico II", Department of Industrial Engineering  
Aerospace Division, Italy

**Giancarlo Troise**  
SEAPOWER Scarl, consortium with University of Naples "Federico II", Italy

## references

- [1] M. McCormick, Ocean Engineering Wave Mechanics, Wiley-Interscience, 1973.
- [2] M. McCormick, Ocean Wave Energy Conversion, Dover Publications, 2007.
- [3] G. De Backer, Hydrodynamic Design Optimization of Wave Energy Converters Consisting of Heaving Point Absorbers, Ghent University, 2009.
- [4] H.O. Berteaux, Buoy Engineering, Wiley-Interscience, 1976.
- [5] T. Matsuoka, K. Omata, H. Kanda, K. Tachi, A Study of Wave Energy Conversion Systems Using Ball Screws - Comparison of Output Characteristics of the Fixed Type and the Floating Type, Proceedings of The Twelfth International Offshore and Polar Engineering Conference, 2002.
- [6] O.M. Faltinsen, Sea loads on ships and offshore structures, Cambridge University Press, 1990.
- [7] G. Payne, Guidance for the experimental tank testing of wave energy converters, SuperGen Marine, 2008.
- [8] CD-adapco, User Guide STAR-CCM+ version 7.06, 2012.